

Different Conformation of Thiol Protease Inhibitor During Amyloid Formation: Inhibition by Curcumin and Quercetin

Mohd Shahnawaz Khan · Abdulrahman M. Al-Senaidy ·
Medha Priyadarshini · Aaliya Shah · Bilqees Bano

Received: 26 August 2012 / Accepted: 7 January 2013 / Published online: 22 January 2013
© Springer Science+Business Media New York 2013

Abstract Cystatins are thiol proteinase inhibitors ubiquitously present in mammalian body and serve various important physiological functions. In the present study, we examined the effects of acid denaturation on newly identified thiol protease inhibitors from the lungs of *Capra hircus* (Goat) with a focus on protein conformational changes and amyloid fibril formation. Acid denaturation as studied by CD (Circular Dichroism) and fluorescence spectroscopy showed that purified inhibitor named GLC (Goat Lung Cystatin) populates three partly unfolded species, a native like state at pH3.0, a partly unfolded intermediate at pH2.0, and unstructured unfolded state at pH1.0, from each of which amyloid like fibrils grow as assessed by thioflavin T (ThT) spectroscopy. The result showed, native like structure formed at pH3.0 is more responsive towards amyloid formation when compare to other conformation of proteins. Morphology of the protein species incubated for amyloid process was observed using transmission electron microscopy (TEM). Moreover, anti-fibrillogenic effects of curcumin and quercetin were analysed using ThT binding assay. Curcumin and quercetin produced a concentration dependent decline inThT fluorescence suggesting deaggregation of the fibrils. When added prior to amyloid fibril initiation 50 μ M curcumin inhibited amyloid aggregation. However, more quercetin is needed to prevent the same extent of fibrillation. Implications for therapeutics in view of polyphenols as essential nutrients are suggested in lung diseases.

Keywords Thiol protease inhibitor · Goat lung cystatin · Amyloid · ThT fluorescence · Electron Microscopy

Introduction

Protein misfolding and aggregation are associated with aging, as well as a variety of human diseases, including Parkinson's disease, cystic fibrosis, amyotrophic lateral sclerosis (ALS), short chain acyl-CoA dehydrogenase (SCAD) deficiency and hypertrophic cardiomyopathy [1–5]. Further, pathogenic depositions of proteins in the form of amyloid like fibrils claim the cause of a number of human diseases. These include Alzheimer's disease, type II diabetes, and spongiform encephalopathies such as Creutzfeldt-Jakob disease [6–8]. In recent years, several non-pathogenic proteins and peptides have been shown to form amyloid fibrils in- vitro including acylphosphatase, cold-shock protein, hen lysozyme, B1 domain of protein G, SH3 domain, cytochrome C, myoglobin [9–15], and pancreatic cystatin [16].

The amyloid fibril usually initiate from partially folded intermediates or molten globules existing under abnormal physiological conditions (like acidic pH, xenobiotic stress, etc.) [17–19]. These intermediate states may escape to serve as initiation points for assembly of aggregates and or amyloid fibrils [16]. The ability to fibrillate is independent of the original native structure of the protein, whose amino acid sequence primarily appears to play a key role in terms of filament arrangement [20], fibrillation kinetics [9], overall yield and stability of the fibrils [8, 21, 22].

Cystatins or thiol proteinase inhibitors are a group of evolutionary related proteins collectively placed in the cystatin superfamily divided into three main groups the stefins, the cystatins and the kininogens depending on the presence of single or multiple 'cystatin domains', presence or absence of a signal sequence, carbohydrate content and sulphhydryl

M. S. Khan · A. M. Al-Senaidy
Department of Biochemistry, College of Science, Protein Research
Chair, King Saud University, Riyadh, Saudi Arabia

M. Priyadarshini · A. Shah · B. Bano (✉)
Department of Biochemistry, Faculty of Life sciences, A.M.U,
Aligarh 202002 U.P, India
e-mail: basiddiqui@hotmail.com

groups. Cystatins constitute a powerful regulatory system for cathepsins, besides this a plethora of biological activities are now ascribed to them [23]. Members of this family show predisposition for fibrillation and have recently been proven to be useful model system to study amyloidogenesis [16, 24, 25].

We have recently reported the purification of lung thiol protease inhibitor (GLC-I), a 66.4 kDa monomeric protein from goat lungs [26]. Based on molecular weight, thiol proteinase inhibitory potential, interaction with thiol proteases and kinetic behaviour, GLC-I was found to be a good confederate of cystatin superfamily [26]. However, no report is available on fibrillation of cystatins from mammalian lung. GLC-I thus served as an attractive candidate for studying its possibility of foraying into aggregate amyloid state during acid denaturation.

There is a lack of any potential anti-amyloidogenic agents till date. Polyphenols have been accredited with myriad biological effects [27]. Their anti fibrillation roles have emerged only lately [28]. An analysis of the effects of natural agents like quercetin and curcumin on fibrillation process can open new avenues for the treatment of protein misfolding diseases. Thus, investigation of the effects of these curcumin and quercetin on GLC-I amyloid formation was also taken up.

The work adds to the spectrum of the proteins, than those so far identified in specific diseases, undergoing amyloidogenesis under defined conditions *in vitro*. It may provide an opportunity to optimize the molecular mechanisms forcing proteins to aggregate *in vivo*. The sequence of events delineated *in vitro* can also help in identifying the spots where the process can be blocked. The work also hints at lung disorders being conformational or their probable aggravation by thiol protease fibrillation/aggregation.

Materials and Method

Chemicals

All chemicals, 1-anilinonaphthalene-8-sulphonic acid (ANS), ThT, curcumin and quercetin was obtained from Sigma chemical Co. (St. Louis MO).

Purification of Thiol Protease Inhibitor

Goat lung cystatin (GLC-I) was purified as reported earlier by Khan and Bano [26]. When proteins precipitated after 40–60 % ammonium sulphate saturation were dialyzed and loaded on DEAE-cellulose ion exchange column, two separate protein peaks with papain inhibitory activity were obtained. The major inhibitory peak named as GLC-I was

used in the present study. The purity of GLC-I was checked by native and SDS-PAGE as reported earlier [26].

Conformational Study of the Inhibitor

GLC-I was allowed to undergo acid denaturation by subjecting it to buffers of varying pH range from pH1.0 to pH7.0. The buffers used were 20 mM solution of glycine/HCl (pH1–2.0), sodium acetate (pH3.0–5.0) and sodium phosphate (pH 6.0–7.0). pH measurements were carried on a Metzer Optical Instruments (Pvt. Ltd., India), pH meter model 603 M with a least count of 0.01 pH unit. GLC-I was incubated with the buffer of desired pH at 25 °C and allowed to equilibrate for 4 h before any spectroscopic measurements.

Amyloid Fibril Formation of the Inhibitor (GLC-I)

GLC-I (50 μM) was incubated in buffers of varying pH1.0, 2.0 & 3.0 containing 150 mM sodium chloride and 0.05 % sodium azide. Before incubation each sample was passed through a 0.2 μm filter to remove traces of aggregated material.

Effect of Polyphenols on the Kinetics of Amyloidogenesis

To study the effects of curcumin and quercetin on fibrillation of GLC-I, different concentration of curcumin and quercetin (0–100 μM) were added to the mixture (50 μM GLC-I incubated in buffer of pH3.0 containing 150 mM sodium chloride and 0.05 % sodium azide).

Spectrophotometric Measurements

The protein concentration was determined by the method of Lowry et al. [29]. A stock solution of ANS in distilled water was prepared and concentration was determined using an extinction coefficient of 5,000 $\text{M}^{-1}\text{cm}^{-1}$ at 350 nm [30]. The molar ratio of protein to ANS was 1:50.

Fluorescence Spectroscopy

Fluorescence measurements were made using a Shimadzu spectrofluorimeter modelRF-540 equipped with a data recorder DR-3 at 25 \pm 2 °C in 1 cm path length quartz cell. The protein concentration used in the measurements was 1 μM . The fluorescence was recorded in the wavelength region 300–400 nm after exciting the protein solution at 280 nm for total protein fluorescence. The slits were set at 5 nm for excitation and emission. To determine the hydrophobic surface exposure during acid denaturation, samples were incubated with a 50-fold molar excess of ANS for 5 min at 25 °C in dark, then fluorescence emission spectra were measured from 400 to 600 nm with excitation at 380 nm.

Circular Dichroism Measurements

Circular dichroism measurements were carried out at $25 \pm 2^\circ\text{C}$ on a Jasco spectropolarimeter model J-720 using a Sekonic X-Y plotter (model SPL-430A) with thermostatically controlled cell holder attached to a NESLAB water bath model RTE 110 with an accuracy of 0.10°C . The instrument was calibrated with d-10-camphorsulfonic acid. The spectra were recorded with a scan speed of 20 nm min^{-1} and with a response time of 4 s. The concentration of GLC-I was 0.2 mg/ml and path length was 1 mm. The spectra obtained were normalized by subtracting the baseline recorded for each condition.

ThT Spectroscopy

Five microlitres of the protein solution in which fibrils were growing were dissolved in 600 μl of the ThT buffer (pH7.5, 25 mM phosphate buffer, 20 μM ThT) just before the measurements. Fluorescence measurements were carried out on a shimadzu spectrofluorimeter model RF-540 equipped with a data recorder DR-3 at 25°C . Excitation was at 440 nm and spectra were recorded from 455 to 600 nm [31].

Transmission Electron Microscopy

A 3 μl sample of protein solution was placed and dried for 5 min on formvar coated carbon grids. After excess fluids were micropipetted from the grid surface, the grid was washed with water and stained with 0.3 % aqueous uranyl acetate. Excess stain was removed and the samples were dried at room temperature. The samples were analyzed at 10 kV in a JEM 1010 transmission electron microscope. Images were captured with an AMT digital camera system (AMT, Chazy, NY).

Results and Discussion

Cystatins comprise large family of thiol proteinase inhibitors whose members have shown propensity to form fibrillar aggregates [32]. Lately, various non-pathogenic proteins have been shown to form amyloid fibrils in vitro, such as acylphosphatase, cold shock protein, hen lysozyme, SH3 domain, cytochrome c and myoglobin [14, 15], etc. One of the aims of the present study was to find environment that is sufficiently destabilizing for the native GLC-I to allow it to explore alternative conformations and lock on to the stable β -sheet aggregated state.

Acid induced unfolding of GLC-I was studied by intrinsic fluorescence properties. In its native state GLC-I is characterized by a peak at 325 nm at pH7.0 [26]. Till pH5.0, no change was observed in λ_{max} of emission (Fig. 1a). However, a 9 nm

blue shift was observed at pH3.0. Lowering the pH to 2.0 caused a red shift of 2 nm further followed by a red shift of 4 nm, at pH1.0. Change in λ_{max} was accompanied by quenching of fluorescence intensity (Fig. 1a). The decrease in fluorescence intensity and a blue shift of 9 nm at pH3.0 is indicative of burial of aromatic residues in the hydrophobic core of the protein and formation of a more compact structure. Red shift observed at pH2.0 and 1.0 can be due to slight unfolding of the structure.

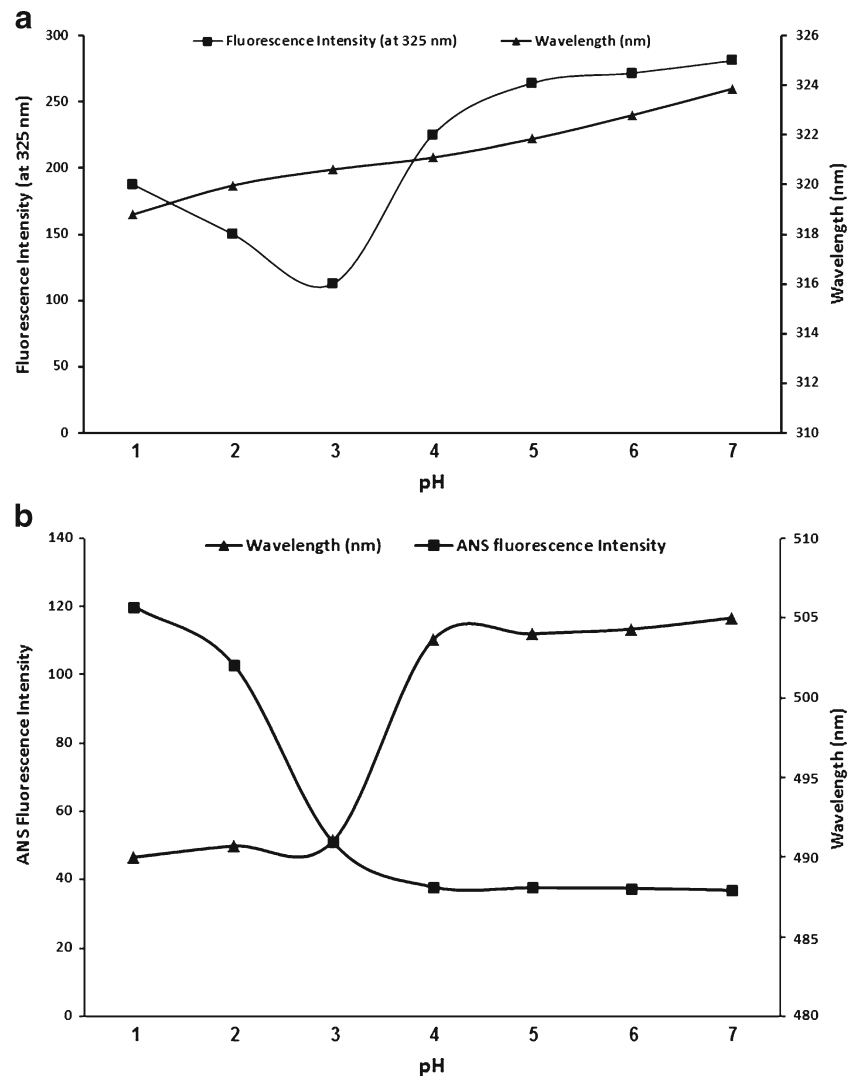
Further, effect of pH on ANS spectrum of purified inhibitor (GLC-I) (Fig. 1b) showed that till pH4.0, there was no appreciable increase in ANS binding suggesting native like structure at pH4.0. A sharp increase was noticeable at pH 3.0. Also, the λ_{max} of ANS-protein complex was blue shifted of 13 nm with no further change on pH reduction. Increase in ANS fluorescence at pH3.0 indicates more hydrophobic residues on protein surface and thus have high propensity to associate through pi-pi interaction.

Perturbation of secondary structure of GLC-I by pH was assessed using circular dichroism. The obtained spectra (Fig. 2) shows decrease in ellipticity at 222 nm below pH 7.0, to a minimum value at around pH3.0. A further decrease in pH below 3.0 resulted in a second transition and shows increase in ellipticity (almost equal to native state) at pH2.0. Thus, inhibitor (GLC-I) at pH3.0 exists a partially unfolded intermediate as shown by transition in ellipticity at 222 nm. GLC-I at pH2.0 exhibit features of an intermediate molten globule like structure with almost native like content of α -helical secondary structure and an enhanced ability to bind ANS dye. (Fig. 1a, b, and 2). While further loss in ellipticity of GLC-I at pH1.0 reflecting unfolding of the inhibitor.

GLC-I when subjected to acid denaturation yields a 'partially unfolded intermediate', the pH3.0 state and a molten globule like intermediate at pH2.0 (Figs. 1 and 2). From these results it is clear that the structure remaining at these low pH values may not be residual native like structure that the acid unfolding has failed to disrupt, but rather newly formed organizations, and consequently with little resemblance to native structure [33]. GLC-I at pH3.0, 2.0 and 1.0 possesses significant non-native secondary structure which is likely to transform to amyloid aggregates. Distinct fibrillar states under differing solution conditions have also been reported for stefin B where different type of fibrils originate from pH4.8-native like and pH3.3-molten globule like intermediate [34].

To prove amyloid formation by purified inhibitor (GLC-I), ThT fluorescence spectroscopy was studied. The enhancement in the fluorescence intensity of ThT upon binding to ordered protein aggregates is a rapid and sensitive method to show presence of fibrils. Free ThT has emission maximum at 450 nm which changes to 485 nm upon binding to fibrils [35]. Changes in fluorescence emission of ThT were monitored at regular time intervals for the incubated samples. The pH3.0 sample, showed a substantial enhancement in ThT fluorescence after

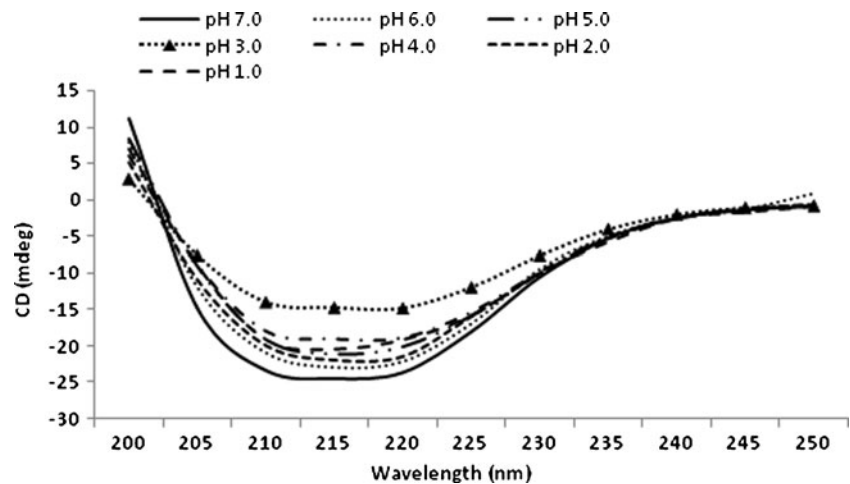
Fig. 1 Intrinsic and Extrinsic fluorescence study of GLC-I at different pH. pH dependence of intrinsic and ANS fluorescence properties of GLC-I. **a** Variation in intrinsic fluorescence intensity at 325 nm and λ_{\max} of emission of GLC-I with pH. GLC-I (1 μM) was incubated in 50 mM solutions of glycine/HCl (pH2.0), sodium acetate (pH3.0–5.0), sodium phosphate (pH6.0–7.0) at room temperature for 4 h. The excitation wavelength was 280 nm and emission was recorded in range of 300–400 nm with a slit width of 5 nm. **b** Variation in ANS fluorescence intensity at 505 nm and λ_{\max} of emission of ANS-GLC-I complex with pH. The samples were prepared as described above. The ANS to protein molar ratio was 1:50. ANS fluorescence was measured at an excitation wavelength of 380 nm in the emission range of 400–600 nm with a slit width of 5 nm



5 days of incubation indicating that at pH3.0 the amyloid growth is rapid (Fig. 3). At pH2.0 however, formation of amyloid proceeds long time as indicated by increase in ThT fluorescence of the same intensity even after 45 days,

suggesting a very lengthy lag phase. GLC-I samples incubated at neutral pH and upto pH4.0 served as controls and showed no ThT binding. GLC-I incubated at pH1.0 also did not give positive for ThT fluorescence. This might be due to

Fig. 2 CD spectra of GLC-I at different pH. For Far UV-CD, 0.2 mg/ml of GLC-I was incubated with tris glycine buffer (pH2.0, 50 mM), sodium acetate buffer (pH3–6.0, 50 mM) and sodium phosphate buffer (pH7.0 and 8.0, 50 mM) for 30 min. at 25 °C and CD spectra were recorded between 190 and 250 nm wavelengths. Cells of 1 mm path length were used



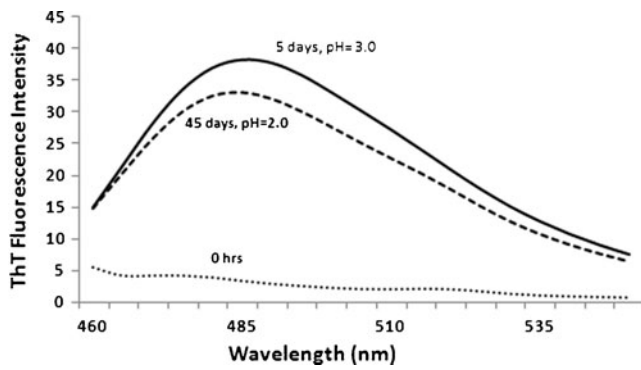


Fig. 3 ThT spectroscopy of GLC-I under acidic pH. Fluorescence emission spectra of thioflavin T (ThT) dye in the presence of goat lung cystatin (50 μ M) incubated with buffers of different pH range varying from (pH1–7) for different interval of time. Five microlitres of the stock solution (protein solution in which fibrils were growing) were dissolved in 600 μ l of the ThT buffer (pH7.5, 25 mM phosphate buffer, 20 μ M ThT) just before the measurements. Excitation was at 440 nm and spectra were recorded between 450–550 nm. The slit width was 5 nm for both excitation and emission beams

disorganization or aggregation of protein molecule at pH1.0. These results thus reveal that amyloid aggregates from GLC form under drastic conditions and more readily at pH3.0.

To further strengthen the corroboration of amyloid formed by GLC-I, transmission electron microscopy (TEM) was performed. Owing to its small size native dehydrated GLC-I gave no distinct image at pH7.0 (Fig. 4). Figure b, shows the TEM image of GLC-I at pH1.0 obtained after 45 days of incubation. Amorphous aggregate like structure is observed. Figure c, shows the TEM image obtained after 45 days of incubation of the sample under similar conditions but at pH2.0. It shows sharp fibrils. Figure d shows TEM images of GLC-I at pH3.0 obtained after 5 days of incubation. Sharp network of fibril is observed. Fibril growth has also been documented under (mild) acidic conditions for insulin [36], endostatin [37], acylphosphatase [9], stefin A [16] and stefin B [17]. Rapid fibrillation of GLC-I was observed at pH3.0 than at pH2.0 and amorphous aggregate like structure is formed at pH1.0; suggesting that unfolded and molten globule like states has a higher propensity to form aggregates. This is supported by reports on fibrillation of bovine serum albumin [38].

Effect of curcumin and quercetin on fibrillization of GLC-I indicates, both curcumin and quercetin reduces the fibrillating potential of GLC-I induced by acidic pH. However, approximately 100 μ M of quercetin is needed to

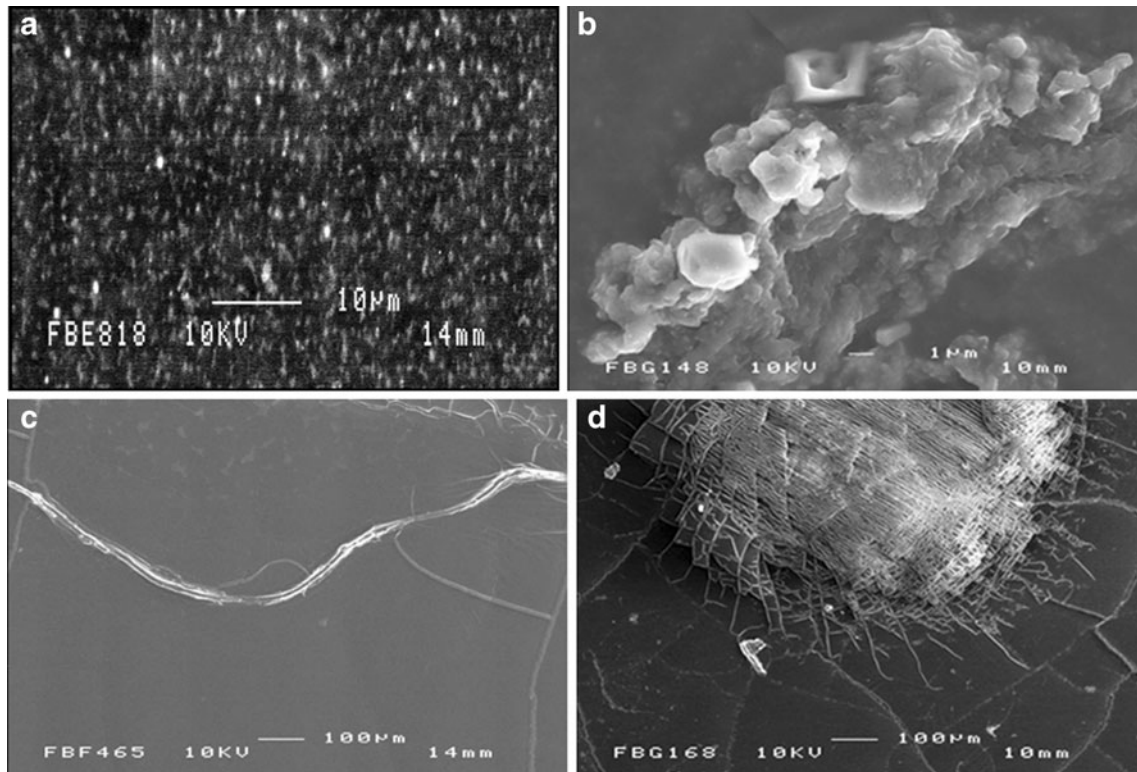
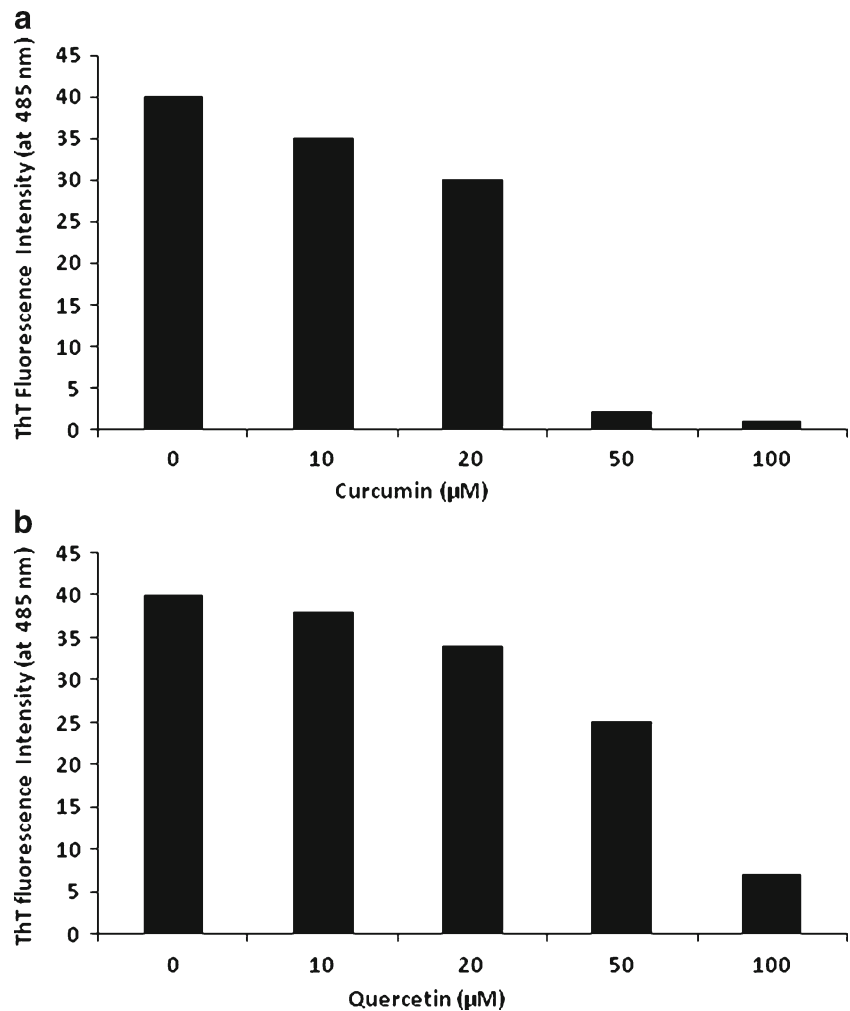


Fig. 4 Electron Microscopy of amyloid making solution of GLC-I at different pH. Electron micrograph of GLC-I incubated under different conditions. **a** Image obtained for GLC-I incubated at pH7.0. **b** Image obtained for GLC-I (at different magnifications as shown by the size of bar lines) incubated at pH1.0 (50 mM glycine/HCl). **c** Image obtained

for GLC-I (at different magnifications as shown by the size of bar lines) incubated at pH2.0 (50 mM glycine-HCl buffer). **d** TEM Image of GLC-I at pH3.0. TEM analysis of all the samples at different pH was obtained after 45 days of incubation

Fig. 5 Effect of curcumin and quercetin on the fibrillation of GLC-I. 50 μ M GLC-I was incubated at pH3.0 in the absence and presence of curcumin and quercetin (0–100 μ M). For ThT assay 5 μ M of incubated sample was used with a protein to ThT molar ratio of 1:6. Excitation was at 440 nm and spectra were recorded at 480 nm with a slit width of 5 nm. The data were obtained after subtraction of the signal of the buffer containing ThT



prevent amyloid, while curcumin does it by only 50 μ M (Fig. 5). The finding is well supported by inhibitory effect of curcumin against hen lysozyme fibrillation [39] and amyloid β oligomers [40]. There are already reports on the quercetin having promising effects on the regression of formation of A β fibrils and disaggregated A β fibrils [41]. The anti-amyloidogenic functionality of polyphenolics is mainly due to its antioxidant, lipid peroxidation and ROS scavenging activity [41].

The findings reported here, along with the previous observation of fibrils formed by SH3 domain [13], BSA [38], stefin B [17], substantiate that amyloid fibril formation is not unique to few proteins found in the amyloid plaques that accumulate in vivo.

Conclusions

The present results suggest that, provided appropriate conditions are maintained over prolonged periods of time, the

formation of ordered amyloid protofilaments and fibrils could be an intrinsic property of many polypeptide chains, rather than being limited to very few aberrant sequences. GLC-I has not yet been implicated as the cause of any diseased state in the lung. However the conditions which predispose it to aggregate may provide an opportunity to understand protein folding better as well as to design therapeutic approaches to combat such an aggregation as deviation from physiological pH under stressful environment may occur in cells. Also, the role of polyphenols in the prevention of aggregation and amyloid would be better tools to design drug/neutraceuticals against conformational protein disorder. Lastly, the experiments further add to the notion that cystatin superfamily members are susceptible to amyloid aggregation.

Acknowledgements The authors extend their appreciation to the deanship of scientific research at KSU for funding the work through the research group project No- RGP-VPP-151.

References

- Schlehe JS, Lutz AK, Pils A et al (2008) Aberrant folding of pathogenic Parkin mutants: aggregation versus degradation. *J Biol Chem* 283:13771–13779
- Luheshi LM, Dobson CM (2009) Bridging the gap: from protein misfolding to protein misfolding diseases. *FEBS Lett* 583:2581–2586
- Winklhofer KF, Tatzelt J, Haass C (2008) The two faces of protein misfolding: gain- and loss-of-function in neurodegenerative diseases. *EMBO J* 27:336–349
- Pedersen CB, Bross P, Winter VS et al (2003) Misfolding, degradation, and aggregation of variant proteins. The molecular pathogenesis of short chain acyl-CoA dehydrogenase (SCAD) deficiency. *J Biol Chem* 278:47449–47458
- Pedersen CB, Kolvraa S, Kolvraa A et al (2008) The ACADS gene variation spectrum in 114 patients with short-chain acyl-CoA dehydrogenase (SCAD) deficiency is dominated by missense variations leading to protein misfolding at the cellular level. *Hum Genet* 124:43–56
- Dobson CM (1999) Protein misfolding, evolution and disease. *Trends Biochem Sci* 24:329–332
- Rochet JC, Lansbury PT (2000) Amyloid fibrillogenesis: themes and variations. *Curr Opin Struct Biol* 10:60–68
- Uversky VN, Fink AL (2004) Conformational constraints for amyloid fibrillation: the importance of being unfolded. *Biochim Biophys Acta* 1698:131–153
- Chiti F, Taddei N, Bucciantini M, White P, Rampovi G, Dobson CM (2000) Mutational analysis of the propensity for amyloid formation by a globular protein. *EMBO J* 19:1441–1449
- Wilkins DK, Dobson CM, Gross M (2000) Biophysical studies of the development of amyloid fibrils from a peptide fragment of cold shock protein B. *Eur J Biochem* 267:2609–2616
- Krebs MR, Wilkins DK, Chung EW, Pitkeathy MC, Chamberlin AK, Zurdo J, Robinson CV, Dobson CM (2000) Formation and seeding of amyloid fibrils from wild-type hen lysozyme and a peptide fragment from the beta-domain. *J Mol Biol* 300:541–549
- Ramirez-Alvarado M, Merkel JS, Regan LA (2000) A systematic exploration of the influence of the protein stability on amyloid fibril formation in vitro. *PNAS* 97:8974–8984
- Zurdo J, Guijarro JI, Jimenez JL, Saibil HR, Dobson CM (2001) Dependence on solution conditions of aggregation and amyloid formation by an SH3 domain. *J Mol Biol* 311:325–340
- Pertinhez TA, Bouchard M, Tomlinson EJ, Wain R, Ferguson SJ, Dobson CM (2001) Amyloid fibril formation by a helical cytochrome. *FEBS Lett* 495:184–186
- Fandrich M, Fletcher MA, Dobson CM (2001) Amyloid fibrils from muscle myoglobin. *Nature* 410:165–166
- Priyadarshini M, Bano B (2012) Conformational changes during amyloid fibril formation of pancreatic thiol proteinase inhibitor: effect of copper and zinc. *Mol Biol Rep* 39:2945–2955
- Rashid F, Sharma S, Baig MA, Bano B (2006) Molten globule state of human placental cystatin (HPC) at low pH conditions and the effects of trifluoroethanol (TFE) and methanol. *Biochem Cell Biol* 84:126–134
- Ahmad B, Khan RH (2006) Studies on the acid unfolded and molten globule states of catalytically active stem bromelain: a comparison with catalytically inactive form. *J Biochem* 140:501–508
- Zerovnik E, Jerala R, Kroon-Zitko L (1992) Intermediates in denaturation of a small globular protein, recombinant human stefin B. *J Biol Chem* 267:9041–9046
- Khurana R, Ionescu-Zanetti C, Pope MLJ, Nielson L, Ramirez-Alvarado M, Regan L, Fink AL, Carter SA (2003) A general model for amyloid fibril assembly based on morphological studies using atomic force microscopy. *Biophys J* 85:1135–1144
- Ahmad A et al (2004) The cellular prion protein PrP^c is expressed in human enterocytes in cell-cell junctional domains. *Biol Chem* 279:1499–15013
- Williams AD, Portelius E, Kheterpal I, Guo JT, Cook KD, Wetzel YX (2004) Mapping abeta amyloid fibril secondary structure using scanning proline mutagenesis. *J Mol Biol* 335:833–842
- Priyadarshini M, Bano B (2010) Cystatin like thiol proteinase inhibitor from pancreas of *Capra hircus*: purification and detailed biochemical characterization. *Amino Acids* 38:1001–1010
- Turk V, Stoka V, Turk D (2008) Cystatins: biochemical and structural properties, and medical relevance. *Frontier Bioscience* 13:5406–5420
- Skerget K, Vilfan A, Pompe-Novak M et al (2009) The mechanism of amyloid-fibril formation by stefin B: temperature and protein concentration dependence of the rates. *Proteins* 74:425–436
- Khan MS, Bano B (2009) Purification, characterization and kinetics of thiol protease inhibitor from goat (*Capra hircus*) lung. *Biochemistry (Moscow Russ Fed)* 74:781–788
- Tyagi S, Singh G, Sharma A (2010) Effect of garlic on cardiovascular disorders: a review. *J Pharm Sci Rev Res* 3:53–55
- Cheng B, Liu X, Gong H, Huang L, Chen H, Zhang X, Li C, Yang M, Ma B, Jiao L, Zheng L, Huang K (2011) Coffee components inhibit amyloid formation of human islet amyloid polypeptide in vitro: possible link between coffee consumption and diabetes mellitus. *J Agric Food Chem* 59:13147–13155
- Lowry OH, Rosebrough NJ, Farr AL et al (1951) Protein measurement with the Folin phenol reagent. *J Biol Chem* 193:265–275
- Mulqueen PM, Kronamn MJ (1982) Binding of naphthalene dyes to the N and A conformers of bovine alpha-lactalbumin. *Arch Biochem Biophys* 215:28–39
- Wang SSS, Liu KN, Han TC (2010) Amyloid fibrillation and cytotoxicity of insulin are inhibited by the amphiphilic surfactants. *Biochim Biophys Acta* 1802:519–530
- Zerovnik E, Skarabot M, Skerget K et al (2007) Amyloid fibril formation by human stefin B: influence of pH and TFE on fibril growth and morphology. *Amyloid* 14:237–247
- LeVine H (1999) Quantification of beta-sheet amyloid fibril structures with thioflavin T. *Methods Enzymol* 309:274–284
- Ahmad A, Uversky VN, Hong D et al (2005) Early events in the fibrillation of monomeric insulin. *J Biol Chem* 280:42669–42675
- He Y, Zhou H, Tang H et al (2006) Deficiency of disulfide bonds facilitating fibrillogenesis of endostatin. *J Biol Chem* 281:1048–1057
- Jenko S, Skarabot M et al (2004) Different propensity to form amyloid fibrils by two homologous proteins-Human stefins A and B: searching for an explanation. *Proteins Struct Funct Bioinf* 55:417–425
- Rabzelj S, Turk V, Zerovnik E (2005) In vitro study of stability and amyloid-fibril formation of two mutants of human stefin B (cystatin B) occurring in patients with EPM1. *Protein Sci* 14:2713–2722
- Holm NK, Jespersen SK, Thomassen LV et al (2007) Aggregation and fibrillation of bovine serum albumin. *Biochim Biophys Acta* 1774:1128–1138
- Wang SSS, Liu KN, Lee WH (2009) Effect of curcumin on the amyloid fibrillogenesis of hen egg-white lysozyme. *Biophys Chem* 144:78–87
- Yang F, Lim GP, Begum AN, Ubeda OJ, Simmons MR, Ambegaokar SS, Chen PP, Kaye R, Glabe CG, Frautschy SA, Cole GM (2005) Curcumin inhibits formation of amyloid beta oligomers and fibrils, binds plaques, and reduces amyloid in vivo. *J Biol Chem* 280:5892–5901
- Davinelli S, Sapere N, Zella D, Bracale R, Intrieri M, Scapagnini G (2012) Pleiotropic protective effects of phytochemicals in Alzheimer's disease. *Oxid Med Cell Longev*. doi:10.1155/2012/386527